Acta Cybernetica — *online–first paper version* — pages 1–23.

On Propagating Uncertainties for Estimation and Association using Validated Interval Simulation

Elliot Brendel[ab], Julien Alexandre dit Sandretto[cd], and Charlotte Govignon[ef]

Abstract

We present a new uncertainty propagation algorithm based on interval arithmetic. The goal is to explore the benefits of a set-based approach for estimation and data association using validated simulation. The presented algorithm capitalises on the measures of a dynamical system to improve its estimation and reduce uncertainties on its trajectory. Our approach also contributes to data association by computing the precision required for a measure to belong to a given track with confidence levels. Mainly interested in space surveillance, we illustrate the contributions of this new algorithm with several scenarios of orbit determination and satellite tracking and their numerical simulations.

Keywords: estimation, association, potential clouds, validated simulation, satellite tracking

1 Introduction

Estimation and association are crucial steps needed in various critical applications such as robotics, autonomous vehicles and radar surveillance. When a set of measures is provided with the respective uncertainties, the estimation problem consists in using this information to compute the state of a dynamical system of interest, for example its position and velocity coordinates. Usually, uncertainties on this estimated state are also computed. Estimation techniques which minimize the state's uncertainties, for instance in terms of Cramér-Rao bound, are often chosen rather than less accurate ones. The estimation accuracy can also be improved by the

[a]Thales Land and Air Systems, Paris, France
[b]E-mail: elliot.brendel@thalesgroup.com, ORCID: 0000-0002-0458-4993
[c]ENSTA Paris, Institut Polytechnique de Paris, 828 Boulevard des Maréchaux, Palaiseau 91120, France
[d]E-mail: julien.alexandre-dit-sandretto@ensta-paris.fr, ORCID: 0000-0002-6185-2480
[e]École des Ponts ParisTech, Cité Descartes, 6 et 8 avenue Blaise Pascal, 77420 Champs-sur-Marne, France
[f]E-mail: charlotte.govignon@ponts.org, ORCID: 0009-0003-7703-0785

DOI: 10.14232/actacyb.314226

simulation of the considered dynamical system, which often requires computing the solution of a differential equation representing its dynamics. When multiple systems evolve in the observed environment, the sensor providing the measures can produce data coming from different objects. Then, filtering of the measures between those coming from the system of interest and the rest is mandatory to prevent the estimate from corruption. This problem is called association. In this paper, estimation and association techniques are presented with a focus on dealing with dynamical systems subject to potentially large uncertainties (such as low-earth satellites), while providing guarantees and confidence levels on the computed results and constraining conservatism.

Data association techniques can be divided in two categories. First, delayed decision techniques wait until several measures are received to perform an association using the set of the measures. For example, Multi-Hypothesis Tracking (MHT) [5, 17] approaches consist in building and updating a set of association hypotheses until their respective estimated probabilities lead to the removal of one of the previous hypotheses. These techniques are efficient but show high combinatorial cost, which can lead to a long time before decision, and can be a drawback in an operating environment. Many other delayed decision approaches consist in the combination of gating [6] and estimation [13, 19, 20] steps. A gating step consists in the selection of a subset of measures satisfying a condition (e.g. all the measures whose distance with the estimate is under a chosen threshold). Then, estimation methods, such as Extended Kalman Filter [5, 13, 19, 20] or Least Squares optimization [10, 19, 20] perform an update of the estimate with the subset of previously selected measures. At last, the new estimate is used to realize a final gating step, and the new selected measures are considered as associated with the object.

Instantaneous decision techniques allocate a measure to an object at the time when, or very shortly after, the measure is received. In these techniques, Nearest Neighbor (NN) [5] methods consist in allocating the considered measure to its closest object by computing a chosen quantity representing a distance between the measure and the objects in its environment. These quantities can be deterministic (e.g. the Cartesian distance) or statistical (e.g. the Mahalanobis distance [20]). When multiple measures and multiple objects are considered at the same time, Global Nearest Neighbor (GNN) methods [5] perform optimization algorithms, such as the Hungarian method [14], to maximize association scores between measures and objects. In general, when the number of measures and objects increases, NN and GNN's efficiency decreases. Probabilistic Data Association (PDA) [3, 5, 8] techniques are instantaneous decision techniques performing the computation of the probability of each association hypothesis and the selection of a subset of these hypotheses. Then, a combination of the selected hypotheses is computed, allocated to an object and used to improve its estimate. This approach is usually suitable for environments with multiple objects and risk of confusion.

Most of the described association techniques are probabilistic approaches which are often based on the hypothesis that Gaussian distributions describe well enough the considered uncertainties (from the measures and the estimates) all along the trajectories of the observed objects. However, in multiple documented examples

such as satellite tracking [11], a Gaussian distribution propagated along a trajectory can lose its Gaussian nature, in particular with large uncertainties, which can happen when the tracked object generated a limited number of measures. The previously presented methods then become unsuitable. Conversely, deterministic set-based propagation and association approaches, using classical set theory functions such as intersection, inclusion and contractors, provide a guaranteed enclosure of all the possible values of the objects states. The obtained enclosures can be used to decide, with guarantee, if a measure belongs to an object or not.

The main tool used for deterministic association and state estimation is the well known interval arithmetic (IA). For example, the latter has been applied to the localization of a robot in [12]. In real world, measures come with uncertainties, but in some cases they can be completely wrong. This is the problem of outliers. They must be carefully handled. With IA, the relaxed intersection is efficient for the outlier management as in [7, 12]. In this paper, we focus on dynamical objects (satellites) and thus, an approach handling dynamics is required. In [18], a method for data association and state estimation with dynamics has been proposed. However, all these techniques require continuous, frequent or regular observations of landmarks, which is not the case of stallites tracking. Observations are rare and tracking is highly uncertain. If IA based techniques seem relevant in a space surveillance context, some new methods are needed. The approaches developed in this paper are applied to association, estimation and tracking of satellites observed by a ground radar. Performances and benefits of these approaches are discussed in connection to this space surveillance application. Indeed, classical IA techniques for the propagation of uncertain trajectories will provide a too large approximation, because of the long time between observations of a satellite by a radar, due to Earth revolution and the dynamics of satellites. The result will not be usable for discrimination between two satellites. To deal with this issue, we propose a confidence-based approach that allows us to make varying the well known conservatism associated with IA.

Section 2 provides preliminary notions required in this paper. Our approach for estimation and association from rare and uncertain measures is presented in Section 3. Then, Section 4 presents numerical results for the simulation in four different scenarios. Conclusion and perspectives are given in Section 5.

2 Preliminary Notions

One of the most used tool to handle bounded uncertainties is the interval arithmetic. In this section, we present the notions used in the paper.

2.1 Interval arithmetic

An interval $[a] = [\underline{a}, \overline{a}]$ defines the set of $a \in \mathbb{R}$ such that $\underline{a} \leq a \leq \overline{a}$. $\mathbb{IR}$ denotes the set of all intervals over $\mathbb{R}$. Usual mathematical operators are extended to intervals: $[a] * [b] = \{a * b \,|\, a \in [a], b \in [b]\}$ with $*$ a binary operator on real numbers. Such

operations can sometimes be expressed via the bounds of the intervals, but not always. For instance, the sum of two intervals $[a]$ and $[b]$ gives $\left[\underline{a}+\underline{b}, \overline{a}+\overline{b}\right]$, but the division of an interval $[a]$ by an interval $[b]$ gives different expressions depending on interval $[b]$ containing 0 or not. Elementary functions can also be extended to interval arithmetic. A *tube* denotes the image of a function $f : t \in \mathbb{R} \mapsto [f(t)] \in \mathbb{IR}$. The Cartesian product of n intervals is called an interval vector or a *box* $[a] \in \mathbb{IR}^n$.

An *interval contractor* associated with the set $A \subset \mathbb{R}^n$ is an operator $C : [a] \in \mathbb{IR}^n \mapsto C([a]) \in \mathbb{IR}^n$ satisfying the contractance property $C([a]) \subseteq [a]$ and the correctness property $C([a]) \cap A = [a] \cap A$. Associated with a *constraint*, a contractor allows to reduce the size of an interval while preserving the subset of real numbers verifying the constraint.

2.2 Validated Simulation

Numerical integration consists in approximating a solution of an ordinary differential equation (ODE), $\dot{x} = f(x)$, using an integration scheme (such as Euler or Runge-Kutta). Interval arithmetic can be applied to numerical integration to provide validated numerical integration methods, also named reachability analysis or guaranteed simulation.

Such validated integration methods use guaranteed integration schemes, providing a discretization of time, $t_0 \leqslant \cdots \leqslant t_{\text{end}}$, and a computation of enclosures of the set of states of the system $x_0, \ldots, x_{\text{end}}$.

A guaranteed integration scheme consists in an integration method $\Phi(f, x_j, t_j, h)$, approximating the exact solution $x(t_{j+1}; x_j)$, i.e., $x(t_{j+1}; x_j) \approx \Phi(f, x_j, t_j, h)$, where x_j is an initial value, t_j the initial time, and h the step-size ($t_{j+1} = t_j + h$), and a truncation error function $\text{LTE}_\Phi(f, x_j, t_j, h)$, such that $x(t_{j+1}; x_j) = \Phi(f, x_j, t_j, h) + \text{LTE}_\Phi(f, x_j, t_j, h)$.

Taking into account the approximation of the used integration scheme, in contrast with usual integration methods, a validated numerical integration method is a two-step method which, firstly, computes an enclosure $[\widetilde{x}_j]$ of the solution over the time interval $[t_j, t_{j+1}]$ to bound $\text{LTE}_\Phi(f, x_j, t_j, h)$, then, computes a tight enclosure of the solution for the final time instant t_{j+1}. Multiple methods exist to perform these steps, such as Taylor series and Runge-Kutta, see [2, 15] and the references therein for more details. The step-size can be fixed (h is a constant) or adaptive. Finally, functions R and $\widetilde{R}$ are provided by validated numerical integration methods

$$R : \left\{ \begin{array}{ccc} \mathbb{R} & \to & \mathbb{IR}^n \\ t & \mapsto & [x] \end{array} \right. , \ \widetilde{R} : \left\{ \begin{array}{ccc} \mathbb{IR} & \to & \mathbb{IR}^n \\ [\underline{t}, \overline{t}] & \mapsto & [\widetilde{x}] \end{array} \right. \tag{1}$$

which for a given t_i, $R(t_i) = \{x(t_i; x_0) : \forall x_0 \in [x_0]\} \subseteq [x]$, and $\widetilde{R}([\underline{t}, \overline{t}]) = \{x(t; x_0) : \forall x_0 \in [x_0] \wedge \forall t \in [\underline{t}, \overline{t}]\} \subseteq [\widetilde{x}]$.

2.3 Confidence Contractor

Intervals and probabilities are strongly connected. Indeed, the universe of a distribution is an interval, and a given confidence level is associated with a confidence

interval. A *confidence interval* is a set $\mathcal{S}$ for which the probability of the given random variable to be in this set is equal to a given probability P. In other words, let $\widehat{x}$ be a single observed sample of a quantity X. In statistics, an observed data allows to compute a confidence interval [16], that is to say an interval which may contain the actual value, with respect to a given confidence level. For example, considering a confidence level CL = 95%, one can define the confidence interval $C_{95\%}$. This interval can be obtained by observation (statistical approach) or with the help of a known distribution (probabilistic approach). A new measure $\widehat{x}$ coming from the (same) experiment will be in the associated confidence interval such that $\widehat{x} \in C_{95\%}$ 95% of the time.

We use in our algorithm the confidence contractor proposed in [1]:

$$\begin{array}{rccc} Cbc([x]|f_X, \text{cc}) : \mathbb{IR} & \rightarrow & \mathbb{IR} \\ [x] & \mapsto & [x] \cap [y] \end{array} \tag{2}$$

with $[y]$ defined such that $Pr(x \in [y]) = \int_{[y]} f_X(x)\, dx = \text{cc}$ ($[y]$ is the confidence interval), $Pr(x \in [y])$ stands for "probability that x is in $[y]$", with x following the distribution f_X, and cc being the confidence coefficient ($0 \leq \text{cc} \leq 1$). For example, cc = 0.68 for a 68% confidence level. In the domain of ODEs, confidence contractor has been used to produce potential clouds [9] in [1]. A potential cloud obtained from the validated simulation of an ODE is a set of reachable tubes computed from the most conservative initial states (the support) to the less one (the mean).

3 Association and Estimation of Measures

Based on interval arithmetic and validated simulation, our approach uses measures of the observed object's state to improve the estimation of its trajectory and rule out incompatible measures and tracks, where a track is a set of measures associated together and the corresponding state estimate and uncertainties.

3.1 Definition of Measures

Measuring instruments or sensors provide measures and their corresponding uncertainties, in either a deterministic (3) or a probabilistic (4) approach. In the deterministic case, the measure $x_{\text{mes}} \in \mathbb{R}^n$ and uncertainty $\Delta x_{\text{mes}} \in \mathbb{R}^n_+$ generate an interval vector that necessarily includes the true quantity x_{true}:

$$x_{\text{true}} \in [x_{\text{mes}} - \Delta x_{\text{mes}}, x_{\text{mes}} + \Delta x_{\text{mes}}]. \tag{3}$$

In the probabilistic approach, the measure is represented as a random variable X_{mes} normally distributed with mean x_{true} and covariance $P \in \mathbb{R}^{n \times n}$:

$$X_{\text{mes}} \sim \mathcal{N}(x_{\text{true}}, P). \tag{4}$$

In the probabilistic approach, the uncertainty is carried by the covariance matrix P. The probabilistic approach is often preferred to represent uncertain measures.

However, the downside of this model is its lack of accuracy to describe rare events and singularities that have a low probability to be drawn. In contrast, the deterministic, or set-based approach, allows to take the entire measure interval into consideration, which is significantly more robust with worst case scenarios. For this reason, we choose to consider measures as real valued intervals.

When sensors provide probabilistic uncertainties, a conversion from the uncertainty covariance P to a deterministic uncertainty Δx_{mes} can be performed (see Subsection 4.2).

3.2 Estimation with Interval Measures

In an ideal case, complete observation of the system is provided. However, it is often impossible (e.g. position is measured but not velocity), therefore a more realistic case has to be considered with an only partial observation of the system.

3.2.1 Complete Observation of the System

A dynamical system of state $x_{\text{true}}(t) \in \mathbb{R}^n$ at time $t \in \mathbb{R}$, following the dynamics $\dot{x}_{\text{true}} = f(x_{\text{true}})$ with $f : \mathbb{R}^n \to \mathbb{R}^n$ is considered. The state is measured with a deterministic approach, as in (3).

From the sensor point of view, measures of the dynamical system with their corresponding uncertainties provide an enclosure of the state. At time t, the measure $x_t^m \in \mathbb{R}^n$ and its corresponding uncertainty $\Delta x_t^m \in \mathbb{R}_+^n$ are received, and lead to the following inclusion:

$$x_{\text{true}}(t) \in [x_t^m - \Delta x_t^m, x_t^m + \Delta x_t^m]. \tag{5}$$

From the observed object point of view, validated numerical integration of the dynamical system provides an interval estimate encompassing the state of the system. At time t, the estimate $[\widehat{x}_t]$ of the system is given by:

$$[\widehat{x}_t] := R(t) \in \mathbb{IR}^n, \tag{6}$$

where $R(\cdot)$ is defined in (1), and $R(t_0) = [\widehat{x}_0]$ with $[\widehat{x}_0]$ the initial value of the system estimate, at time t_0. The true state at time t is also included in $[\widehat{x}_t]$:

$$x_{\text{true}}(t) \in [\widehat{x}_t]. \tag{7}$$

Using (5) and (7), the state of the dynamical system is included in the intersection of the measure and the estimate:

$$x_{\text{true}}(t) \in [x_t^m - \Delta x_t^m, x_t^m + \Delta x_t^m] \cap [\widehat{x}_t]. \tag{8}$$

Furthermore, if the exact time $t \in \mathbb{R}$ of the measure is not known precisely, it can be approximated by a time interval. Assuming that the exact time t is bounded by $\underline{t} \leq t \leq \overline{t}$, then instead of using $R(\cdot)$ to provide the estimate as in (6), the function $\widetilde{R}(\cdot)$ generates an estimate $[\widehat{x}_t] := \widetilde{R}(t) \in \mathbb{IR}^n$, taking into account the uncertainty on the time of the measure.

3.2.2 Partial Observation of the System

In some cases, the sensor provide measures from the dynamical system in a different reference frame or partial measures with respect to the state. In this section, it is considered that the sensor can only make observations $y_t^m \in \mathbb{R}^p$ of the system $x_{\text{true}}(t) \in \mathbb{R}^n$, with $p \leq n$. An observation function $g : \mathbb{R}^n \to \mathbb{R}^p$, allowing the conversion of a vector from the state frame to the measure frame, gives the following theoretical constraint for a measure without uncertainty

$$g(x_{\text{true}}(t)) - y_t^m = 0, \tag{9}$$

which represents the compatibility of the system x_{true} with the measure y_t^m at time t. If a measure y_t^m does not verify this constraint, then it cannot come from the system x_{true}. Further, if the measure y_t^m comes from the system x_{true}, the constraint in (9) provides more information on the state of system $x_{\text{true}}(t)$.

The constraint in (9) can be written as a double inclusion between two singletons: $\{g(x_{\text{true}}(t))\} \subset \{y_t^m\}$ and $\{y_t^m\} \subset \{g(x_{\text{true}}(t))\}$. This last constraint can be written as $\left\{g^{-1}\left(y_t^m\right)\right\} \subset \{x_{\text{true}}(t)\}$ when g is bijective. Therefore, given a partial measure interval $[y_t^m] \in \mathbb{IR}^p$ and an estimated interval $[\widehat{x}_t] \in \mathbb{IR}^n$ of a system at time t, the interval counterpart of (9) is as follows:

$$\begin{cases} g([\widehat{x}_t]) \subset [y_t^m], \\ g^{-1}([y_t^m]) \subset [\widehat{x}_t]. \end{cases} \tag{10}$$

The smallest subset of $[\widehat{x}_t]$ that respects (10) is computed with a forward-backward contractor [4], providing a solution without computing g^{-1}, as g is usually not bijective.

As a result, when the measures are only partial and cannot be used to directly intersect the estimated interval (8), interval contractors allow to use the partial information provided by the measures (10).

3.3 Association of Measures

Association is performed by comparing the estimate of a dynamical system with new measures. If the association decision is positive, the estimation step is computed using the information of the measures and their uncertainties to reduce the uncertainty of the estimate. Our algorithm (see Algorithm 1) performs these steps for the complete observation case (see Subsection 3.2.1). A similar algorithm has been implemented for the partial observation case (see Subsection 3.2.2) using (10) instead of (8) as an association rule and improvement of the estimate.

Our algorithm (see Algorithm 1) ensures that a measure is compatible with the simulated dynamical system to perform their association. Since the simulation is validated, the estimated interval vector necessarily includes every possible states of the dynamical system. So, if a measure interval does not intersect with the simulated interval corresponding to the same instant, this necessarily means that the measurement is incompatible with the evaluated track. Nonetheless, it is

possible that certain measures give a non-empty intersection with the simulation estimate, but do not really correspond to the same system. Hence the significance of introducing confidence levels in the measurements.

Algorithm 1 Interval Measure Association with Complete Observation Algorithm.

Funct IMACO($[\widehat{x}_t]$, x_t^m, Δx_t^m)

if $[\widehat{x}_t] \cap [x_t^m - \Delta x_t^m, x_t^m + \Delta x_t^m] \neq \emptyset$ **then** *Association rule*
  Association because of compatibility
  Improvement of the estimate: $[\widehat{x}_t] \leftarrow [\widehat{x}_t] \cap [x_t^m - \Delta x_t^m, x_t^m + \Delta x_t^m]$ (8)
else
  Incompatibility, no association
end if
return $[\widehat{x}_t]$ and association decision

---

for some values of confidence $0 < \mathrm{cc}_i < 1$ **do**
  Compute $[\widehat{x}_t]_{\mathrm{cc}_i}$
  IMACO($[\widehat{x}_t]_{\mathrm{cc}_i}$, x_t^m, Δx_t^m)
end for

Once the algorithm ruled out incompatible measures, it uses the additional information of the measure to increase the precision on the state of the dynamical system using Section 3.2. This gives an upgrade of the estimate by reducing the uncertainty on the state of the system after the measure.

4 Application to Satellite Tracking

Space surveillance of low-earth objects has become a major challenge, notably in a military context. It can be addressed by ground radars, providing detection and tracking of satellites of interest. Estimation and association are crucial steps for the tracking of these objects.

It is important to notice that a ground radar can only provide measures for low-earth satellites when these objects are in its field of view. Therefore, due to earth rotation and satellite dynamics (see Subsection 4.1.2), measures of an observed satellite can be spaced out by several hours. This potentially important time range between measures can cause a loss of precision in the estimate of the satellite state, leading to increased uncertainties and, possibly, confusion with other objects. Moreover, the fact that a Gaussian distribution propagated along an orbital trajectory can lose its Gaussian nature [11] has been documented, in particular when uncertainties are large, for instance when the object generated a limited number of measures.

Therefore, the deterministic set-based propagation and association approaches developed in this paper can be relevant in a space surveillance context, allowing to relax the Gaussian hypothesis. In this section, useful preliminary notions of orbit determination are presented. Then, in order to demonstrate the benefits of our

approach in various substeps of the tracking task, our approach is studied through propagation, estimation and association scenarios. Finally, the performances of our approach are compared to a probabilistic NN method in a propagation and association scenario.

4.1 Preliminary Notions of Orbit Determination

4.1.1 Orbit Description

The state of a dynamical system can be given with its vectors of position and velocity. For a satellite, these six coordinates can be expressed in earth-centered Cartesian references such as *Earth-Centered Intertial* (ECI) or *Earth-Centered Earth-Fixed* (ECEF). Alternatively, it can be convenient to describe a satellite state in the *Keplerian* or the *Equinoctial* frames [19], especially when the dynamics are unperturbed, since these frames provide a more direct handling of the parameters of the ellipse. *Modified equinoctial elements* [21] (mEOE) are derived from Keplerian elements $(a, e, i, \Omega, \omega, \theta)$ as follows:

$$\begin{cases} p = a\left(1 - e^2\right), \\ f = e\cos\left(\omega + \Omega\right), \\ g = e\sin\left(\omega + \Omega\right), \\ h = \tan\left(\frac{i}{2}\right)\cos\Omega, \\ k = \tan\left(\frac{i}{2}\right)\sin\Omega, \\ L = \Omega + \omega + \theta, \end{cases} \tag{11}$$

where a denotes the semi-major axis, e the eccentricity, i the inclination, Ω the longitude of the ascending node, ω the argument of the periapsis, θ the true anomaly. The element p is called the semi-parameter and the element L is called the true longitude. This reference is useful for trajectory analysis because of the stability of the state components in time (see Subsection 4.1.2).

4.1.2 Dynamics of a Satellite

The dynamics of a satellite in mEOE is given by (12) [21]:

$$\begin{cases} \dot{p} = \frac{2p}{w}\sqrt{\frac{p}{\mu}}\Delta_t, \\ \dot{f} = \sqrt{\frac{p}{\mu}}\left(\frac{((w+1)\cos L + f)\Delta_t - gj\Delta_n}{w} + \Delta_r \sin L\right), \\ \dot{g} = \sqrt{\frac{p}{\mu}}\left(\frac{((w+1)\sin L + g)\Delta_t + fj\Delta_n}{w} - \Delta_r \cos L\right), \\ \dot{h} = \sqrt{\frac{p}{\mu}}\frac{s^2\Delta_n}{2w}\cos L, \\ \dot{k} = \sqrt{\frac{p}{\mu}}\frac{s^2\Delta_n}{2w}\sin L, \\ \dot{L} = \frac{\sqrt{\mu p}}{r^2} + \frac{1}{w}\sqrt{\frac{p}{\mu}}(h\sin L - k\cos L)\Delta_n, \end{cases} \tag{12}$$

where $w = 1 + f\cos L + g\sin L$, $s^2 = 1 + h^2 + k^2$, and $j = h\sin L - k\cos L$. Δ_t, Δ_r and Δ_n are the non-two-body perturbations in the radial, tangential and normal directions, respectively. These perturbations aggregate all other orbital perturbations acting on the satellite, like the J_k effects ($k \in \{2, 3, ...\}$) which come from the non-sphericity of the Earth, or the atmospheric drag for instance. For low-earth orbit satellites, J_2 effects induce the strongest perturbation. Therefore, the considered perturbations are:

$$\begin{cases} \Delta_r^{J_2} = -\frac{3\mu J_2 R_e^2}{2r^4}\left(1 - \frac{12j^2}{s^4}\right), \\ \Delta_t^{J_2} = -\frac{12\mu J_2 R_e^2}{r^4}\left(\frac{j(h\cos L + k\sin L)}{s^4}\right), \\ \Delta_n^{J_2} = -\frac{6\mu J_2 R_e^2}{r^4}\left(\frac{(1-h^2-k^2)j}{s^4}\right), \end{cases} \tag{13}$$

where J_2 is the second order zonal coefficient, R_e the earth radius, μ the standard gravitational parameter and $r = \frac{p}{w}$ is the radius. Without perturbations, all equinoctial elements are constant except the true longitude L which is close to linear (12).

4.1.3 Satellite Tracking by Ground Radar

The space is periodically scanned by a ground radar trying to detect new satellites. Then, every produced measure is compared to the estimates of known objects in order to decide if the measure was generated by a known object or by a previously unknown one: this is the measure association step. If the measure belongs to a known object, its estimate is updated and improved by the information of the measure. If the measure belongs to a new object, an estimate of this object is computed and the object will be considered as known for the future measures performed by the radar.

4.2 Simulation Hypotheses

In this paper, the considered radar produces measures of the position of detected objects in the ECI frame. This simplification is justified by the fact that measures performed in a Radar frame, such as Azimuth-Elevation-Range, can easily be converted in a Cartesian frame using classical formulas [19].

The measures provided by the radar come with a covariance matrix, also in ECI, representing the uncertainties of the associated measures. Mathematically, each of these measures can be modelled by a random variable $X_{\text{mes}} \in \mathbb{R}^3$ normally distributed with mean $x_{\text{true}} \in \mathbb{R}^3$ (the true position of the satellite in the ECI frame) and covariance $P \in \mathbb{R}^{3\times3}$ (depending on the radar performances and the satellite position), as in (4). The confidence contractor presented in (2) provides measure boxes, as in (3), corresponding to a chosen confidence level (in this paper, 99%).

The presented method has been implemented in the DynIbex framework [2]. It provides interval arithmetic tools such as contractors and offers a validated numerical integration procedure based on Runge-Kutta methods with adaptive step-size. The presented simulations were computed using the *implicit midpoint* method. The tolerance on the local truncation error [2] was set to 10^{-7}. This choice of parameters granted a good trade-off between computation time and precision.

The objects were simulated in the mEOE frame. The semi-parameter p was normalised by the Earth radius and the time unit for the integration was hours instead of seconds to facilitate the computations.

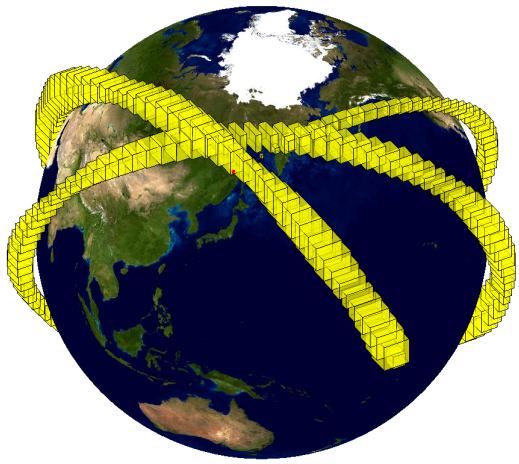

Figure 1: Simulation of a trajectory of a satellite for 6 hours, represented by the boxes of uncertainties on its position, with the starting box in red.

The initial estimate of each simulated satellite is supposed to be normally distributed with a mean vector x_0 and a covariance matrix P. x_0 depends on the scenario. P is common to scenarios 1 to 3 (see Subsections 4.3, 4.4 and 4.5) and chosen diagonal such that $P_{11} = 594.817$, $P_{66} = 1.258 \cdot 10^{-11}$ and $P_{ii} = 5.948 \cdot 10^{-14}$ for $i = \{2, \ldots, 5\}$. This covariance matrix is representative of the uncertainties on the state of a satellite after a few measures. It is satisfactory to demonstrate the contribution of our algorithm but in operating environment, distinct covariance matrices for the satellites of interest would be considered, depending on the measures used to compute their respective estimate, and a given time at which the matrices are evaluated.

Then, a reference box is computed using the confidence contractor of (2) with a 99% confidence level: $\Delta x_{\text{ref}} = [-x_{\text{ref}}, x_{\text{ref}}]$ where $x_{\text{ref},1} = 100$, $x_{\text{ref},6} = 1.45408 \cdot 10^{-5}$ and $x_{\text{ref},i} = 10^{-6}$ for $i = \{2, \ldots, 5\}$. This represents an uncertainty of $[-100, 100]$ meters on the semi-parameter p, and approximately $[-100, 100]$ meters on the arc of circle represented by the true longitude L when the altitude of the satellite is 500 kilometers.

The potential clouds associated with the 5% and 95% confidence levels are given by $\Delta x_{5\%} = 0.21\Delta x_{\text{ref}}$ and $\Delta x_{95\%} = 0.645\Delta x_{\text{ref}}$. Then, with x_0 an initial state of a satellite, the initial box associated with the $n\%$ potential cloud ($n = 5, 95$) is given by $x_0 + \Delta x_{n\%}$.

4.3 Scenario 1: Propagation of Uncertainties

The first scenario consists in the propagation of the 5% and 95% potential clouds of a satellite for 6 hours, using the function R defined in (1).

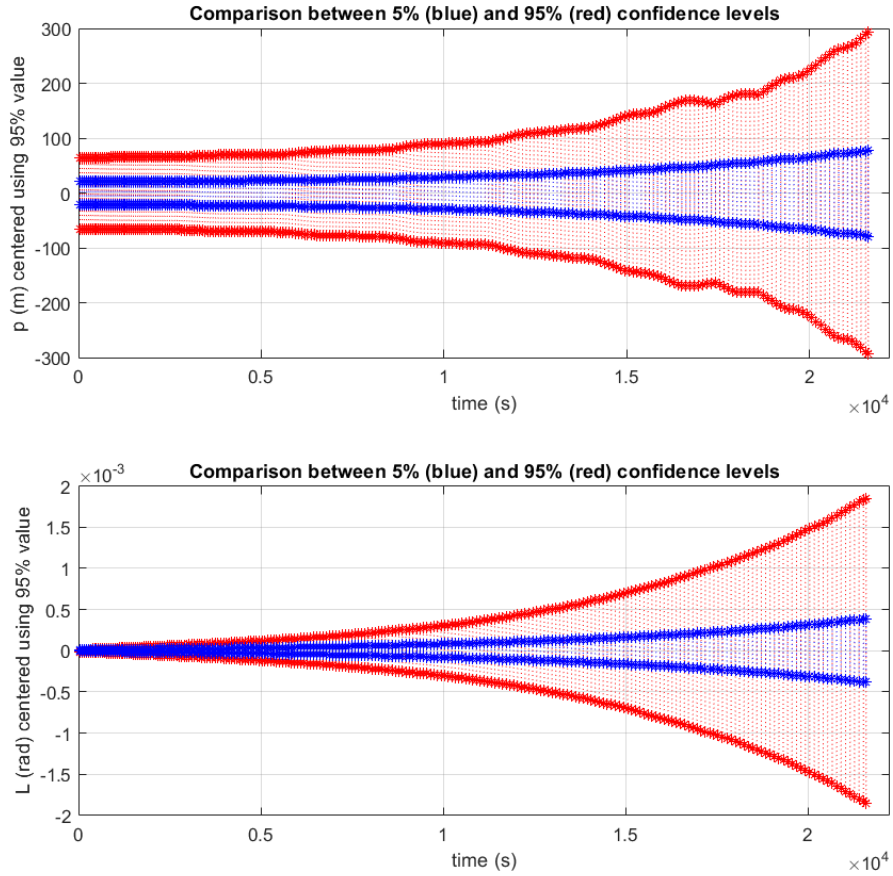

Figure 2: Propagation of the 5% (blue) and 95% (red) potential clouds on the p and L components.

Figure 2 shows the results on the components p and L. For an easier comparison between the two potential clouds, the intervals are translated using the center of the 95% interval. After 6 hours, the 95% potential cloud associated with the semi-

parameter p is about 600 meters wide, three times greater than the 5% potential cloud. Along the propagation, the order of magnitude stays the same for the two potential clouds associated with p. In contrast, the widths of the potential clouds associated with L increase faster and after 6 hours, the circular arcs corresponding to such intervals are about 7 kilometers for the 5% potential cloud and 27 km for the 95% potential cloud. The specificity of the component L is discussed in 4.4. Finally, it can be observed that, as expected, the 5% intervals are always included in the 95% intervals.

4.4 Scenario 2: Effect of Measures on Estimation Uncertainties

In this scenario, a ground radar provided an estimate of the state of the satellite at an initial time, and propagated its estimate for 12 hours with the function R defined in equation (1) before being able to measure its position again. When the satellite gets in the field of view of the radar again, a series of 10 measures of its position over 5 minutes are taken. Using our algorithm, these measures are added to the estimation process.

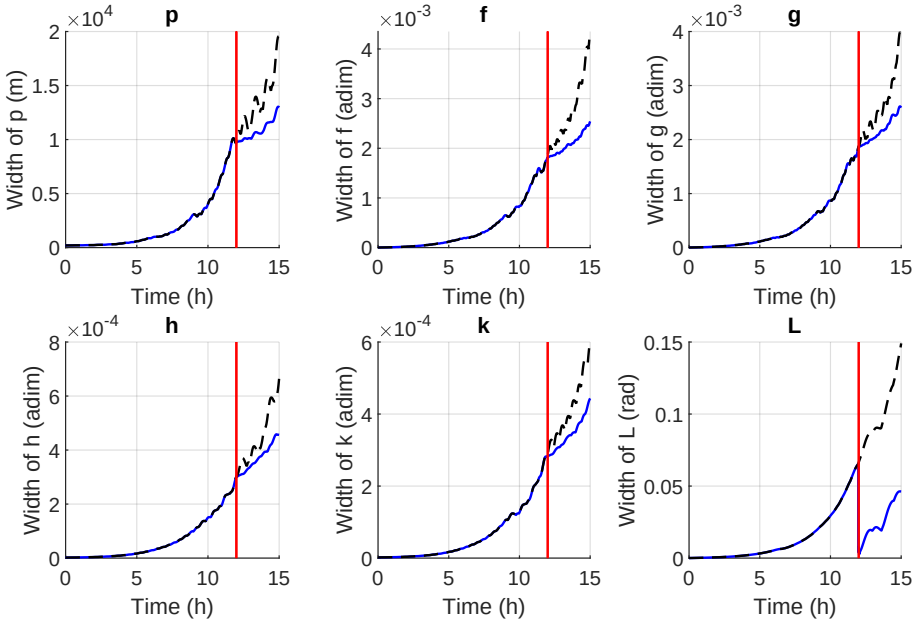

Figure 3: Propagation of the uncertainties, with (blue) and without (black) addition of 10 measures after 12 hours (red).

Figure 3 shows that L is significantly impacted by the series of measures, in comparison to other components of the state of the satellite. Indeed, the uncertainty over L drops with the addition of measures. The precision of the other components

also improves after the addition of measures, compared to the scenario where no measure was added. This comes from the precision gain of L spreading to the other state's components through the dynamics equations.

The impact of the measures on the component L is due to L encoding the position of the satellite along the orbit. Therefore, this component is strongly linked to the position of the satellite, hence the steep decrease of its uncertainties when a position measure is added. Further, the true longitude L is the component which is the most subject to variations over time, since it is the only non-constant one when the dynamics is unperturbed (12). Therefore, it makes the propagated uncertainties grow faster for the true longitude L.

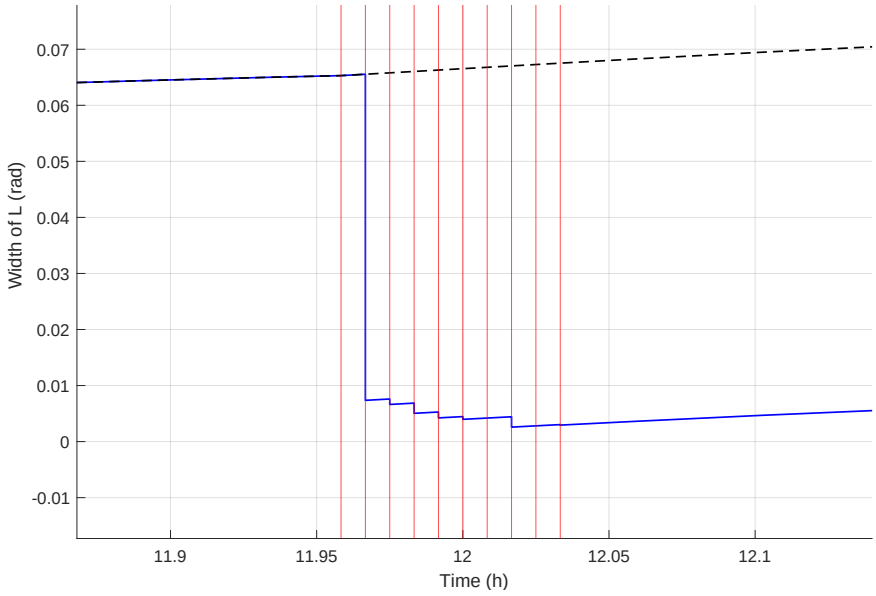

Figure 4: Focus on the effect of each measure on L.

By focusing on the impact of each measure of the series on L, it gives Figure 4, which helps raising two points. First, not every measure helps improving the estimate of the satellite's position. Here, the first measure of the series does not reduce the estimate's uncertainty. Mathematically, it means that the estimation interval was included in the measure interval. The radar is not precise enough to bring new information. Secondly, most of the precision given by the series of measures comes from the first measures. This could allow computing the number of measures that would be necessary to achieve a certain precision on the position of the tracked satellite, depending on the accuracy of the ground radar.

4.5 Scenario 3: Potential Clouds for the Collision Issue and Consequences on Sensor Design

The 5% and 95% potential clouds for two satellites are propagated using validated simulation and the $\widetilde{R}$ function (1) with the initial states:

$$\begin{cases} p_1 = 6890939, & p_2 = 6961989, \\ f_1 = 0.0014125, & f_2 = 0.0014182, \\ g_1 = -0.0014160, & g_2 = -0.0014102, \\ h_1 = 0.57763, & h_2 = -0.57763, \\ k_1 = 0.0095098, & k_2 = -0.0095068, \\ L_1 = -0.32425, & L_2 = -0.31903. \end{cases} \tag{14}$$

At last, the trajectories of the two satellites can be compared as in Figures 5a and 5b. These figures show a sample of the trajectories where the propagated boxes intersect for a 95% confidence level but not for a 5% confidence level. In that respect, the sensor performances can be evaluated in terms of required confidence level and decisions can be made depending on this analysis. These decisions can be design decisions such as improving the sensor's accuracy or multiplying the sources producing measures. In that case, if a sensor can only ensure that a collision will never happen with a 5% confidence level, one can decide to use complementary sources of measures in order to improve the estimation of the satellites states. An other decision could be to maneuver one of the satellites in order to increase the confidence level associated with the collision.

4.6 Scenario 4: Comparison with NN method

In this scenario, two close satellites are considered, but only one of them is the satellite of interest whose state needs to be estimated. Two methods are compared: a NN method [5] whose performance is evaluated with a Monte-Carlo simulation, and a set-based approach using validated simulation and interval arithmetic.

4.6.1 Scenario inputs

The true initial states of the 2 satellites are such that they belong to the same orbit, but satellite 2 is about 200 meters behind satellite 1 on this orbit:

$$\begin{cases} p_1 = 6878130, & p_2 = p_1, \\ f_1 = 0.001, & f_2 = f_1, \\ g_1 = 0, & g_2 = g_1, \\ h_1 = 0.57735, & h_2 = h_1, \\ k_1 = 0, & k_2 = k_1, \\ L_1 = 0, & L_2 = -0.000029078. \end{cases} \tag{15}$$

The estimation step is assumed to produce a normally distributed estimated state $\widehat{x}_1$ of mean $x_1 = (p_1, f_1, g_1, h_1, k_1, L_1)$ and covariance matrix P:

$$\widehat{x}_1 \sim \mathcal{N}(x_1, P), \tag{16}$$

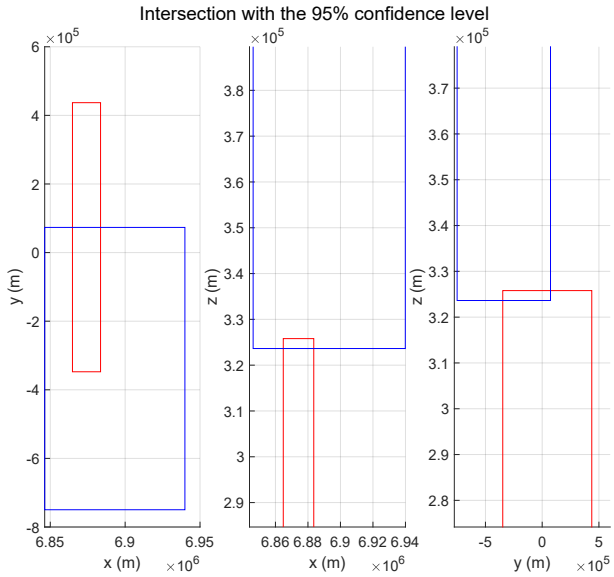

(a) Intersection for 95% potential clouds.

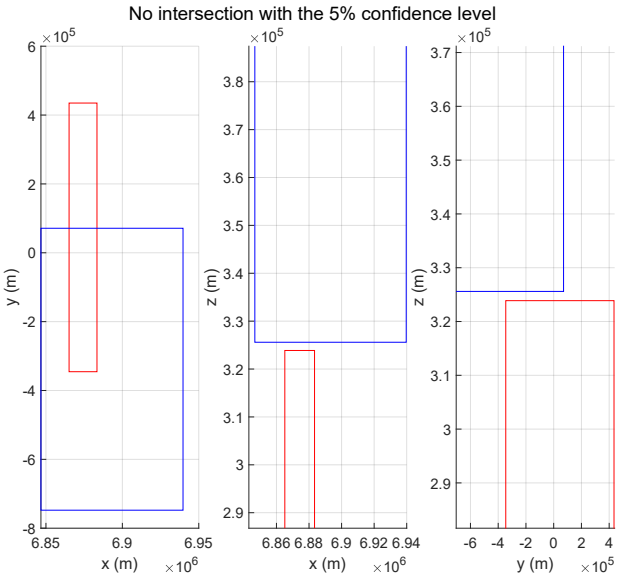

(b) No intersection for 5% potential clouds.

Figure 5: Position boxes at the same time in the ECI frame for the propagation of the 5% and 95% potential clouds of two satellites (blue boxes for satellite 1 and red boxes for satellite 2).

where P is chosen diagonal such that $P_{11} = 594.817$, $P_{66} = 1.258 \cdot 10^{-11}$ and $P_{ii} = 5.948 \cdot 10^{-7}$ for $i = \{2, \ldots, 5\}$. This covariance matrix is representative of the uncertainties on the state of a satellite after a few measures, with amplified uncertainties for $i = \{2, \ldots, 5\}$ in order to enhance the comparison with Monte-Carlo simulation.

4.6.2 NN method and Monte-Carlo simulation

Using (16), 1000 estimated states are randomly drawn and propagated for one hour with a Runge-Kutta method of order 4. The true states of satellites 1 ($x_{1,\text{prop}}$) and 2 ($x_{2,\text{prop}}$) are also propagated using the same method. The covariance matrix P is propagated using the formula

$$P_{\text{prop}} = JPJ^T, \tag{17}$$

where J is the numerically computed Jacobian matrix of the propagation function evaluated at x_1 (as performed in the Extended Kalman Filter [5, 13, 19, 20]). The association metric used to perform the NN method is the Mahalanobis distance [20]. For each simulated estimated state $\widehat{x}^i_{1,\text{prop}}$ and for $j \in \{1, 2\}$, this distance is computed using the formula

$$d^{i,j}_{\text{M}} = \left(x_{j,\text{prop}} - \widehat{x}^i_{1,\text{prop}}\right)^T P^{-1}_{\text{prop}} \left(x_{j,\text{prop}} - \widehat{x}^i_{1,\text{prop}}\right). \tag{18}$$

Then, for each $i \in [1, 1000]$, if $d^{i,1}_{\text{M}} < d^{i,2}_{\text{M}}$, then the ith estimate is associated the the satellite 1. Otherwise, the ith estimate is associated with the satellite 2. The same computations are made in the ECI frame, by converting every state and covariance using the formulas from [21], and (17) with the Jacobian matrix of the conversion function.

Finally, confusion rates are computed: in the mEOE frame, starting from a 0% confusion rate (i.e. every particle is correctly associated with satellite 1), a 20.3% confusion rate is obtained after a one hour propagation (see Figure 6). In the ECI frame, this phenomenon is amplified and the confusion rate is about 83.4% after a one hour propagation (see Figure 7), which means that in a large majority of cases, the NN method would perform the wrong association in this scenario. Considering 10 consecutive measures with these confusion rates, there would only be a 10.3% probability that the batch of 10 measures contains only measures of satellite 1 in the mEOE frame, and 0.0000015% in the ECI frame. Therefore, the estimates of the state of satellite 1 computed with such corrupted batch of measures would be very often corrupted as well.

4.6.3 Set-based approach

The initial states of the two satellites and the estimate of satellite 1 are propagated using validated simulation and the R function (1). The initial states of the two satellites are the same as in (15), with no uncertainty. The initial state of the

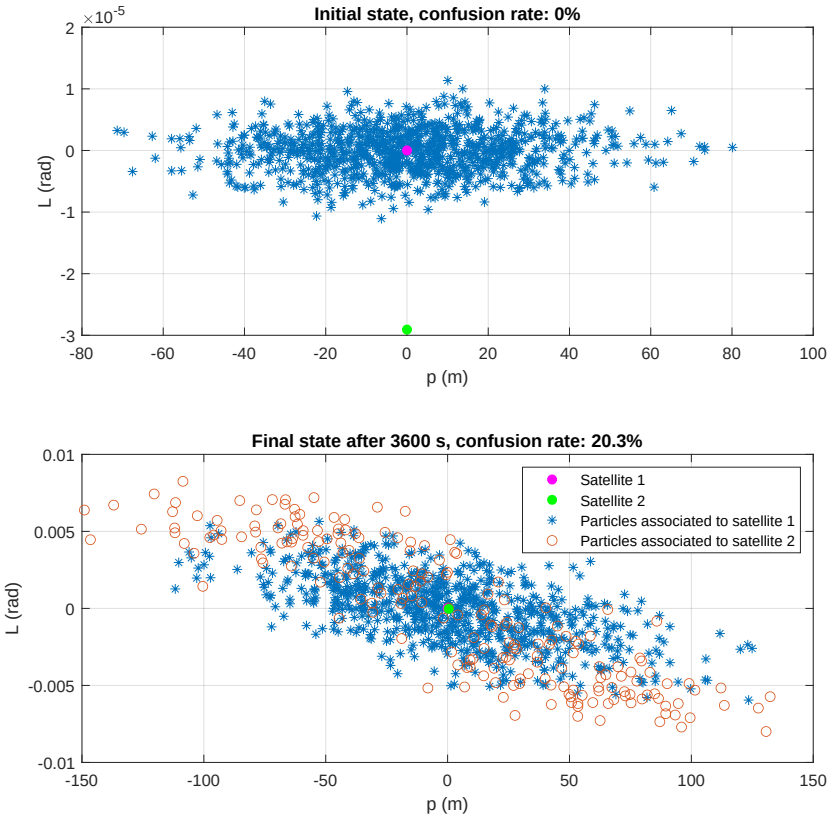

Figure 6: Confusion rate in mEOE after one hour of propagation with 1000 Monte-Carlo simulations.

estimate of satellite 1 is drawn using (16):

$$\begin{cases} \widehat{p_1} = 6878138, \\ \widehat{f_1} = 0.000935524, \\ \widehat{g_1} = -0.001727603, \\ \widehat{h_1} = 0.578592956, \\ \widehat{k_1} = 0.000283935, \\ \widehat{L_1} = 0.000004533, \end{cases} \tag{19}$$

and the corresponding box of uncertainties is computed using the confidence contractor of (2) with a 99% confidence level.

Unlike the NN method which in this case fails to associate the right satellite in about 20% of the Monte-Carlo simulations in mEOE (and 83% in ECI), the box provided by the set-based approach is guaranteed to include the true state

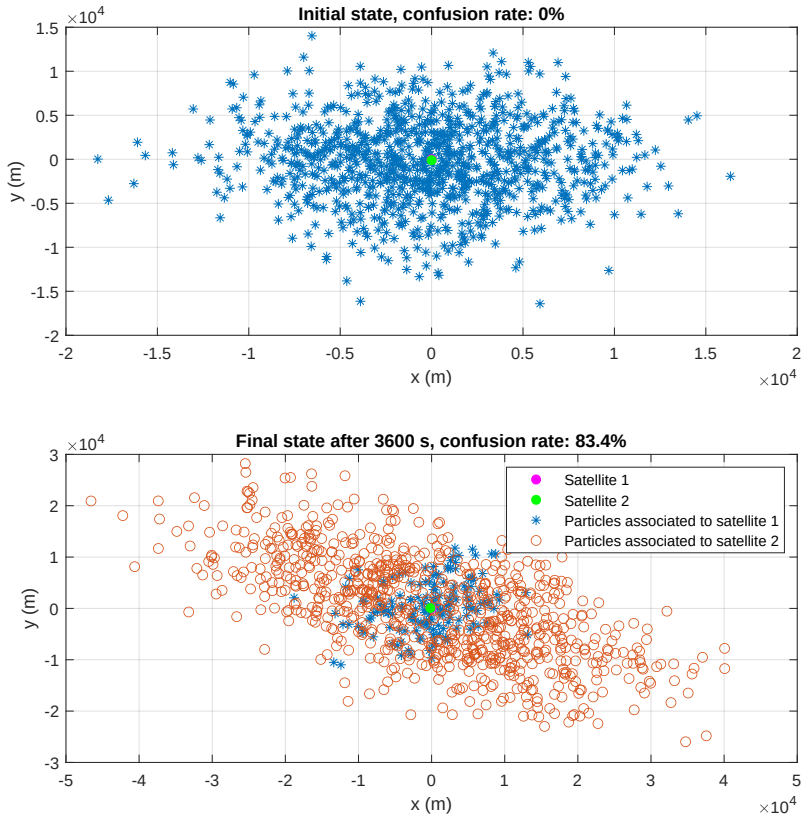

Figure 7: Confusion rate in ECI after one hour of propagation with 1000 Monte-Carlo simulations.

of satellite 1 at least 99% of the time. In this case, both true states of satellites 1 and 2 are included (see Figure 8 and Figure 9) and no association hypotheses can be definitively chosen or left out. However, it is important to keep in mind that multiple measures and backward propagation could enable to decide between these hypotheses with a certain time delay and then improve the accuracy of the state estimate. There is no need to perform a conversion of the tubes from the mEOE frame to the ECI frame here, since the inclusions are preserved by interval arithmetic, Figure 8 and Figure 9 already show that the conclusion would be the same in the ECI frame.

4.7 Discussion

The considered scenarios demonstrate the contribution of our method to various steps of the tracking of low-earth orbit satellites. Scenarios 1 and 3 emphasize

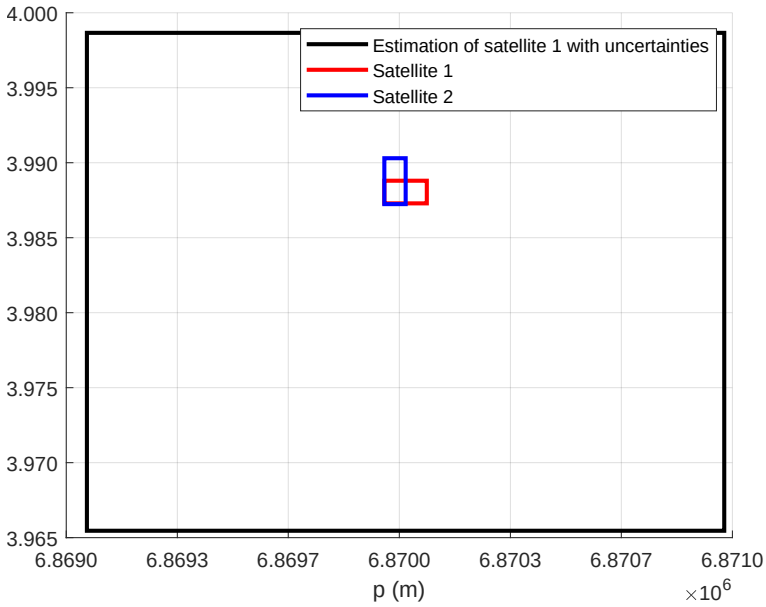

Figure 8: Propagated uncertainty boxes after one hour: satellites 1 and 2 are included in the estimate of satellite 1.

on our ability to compute trajectories of satellites using validated simulation and confidence levels: the prediction step. Scenario 2 shows an association and update step using Algorithm 1. Our set-based approach is compared to a classical NN method in scenario 4, especially in terms of confusion rate, showing the benefits of a set-based approach regarding association decision making in particular.

The missing step for a complete tracking would be the initialization of a track, i.e. the first computation of a satellite state using one or very few measures. Track initialization, also known as initial orbit determination in this context, usually relies on different techniques, such as Gauss's method [19], which remain to be studied and eventually adapted in an interval counterpart.

5 Conclusion and Future Works

In this paper, we proposed a validated approach for association and estimation of dynamical systems, taking account of uncertainties on the initial state, measures and parameters. Our approach uses measures and their uncertainties to quantify likelihood to belong to a certain track. Unlike Monte Carlo methods, our approach provides mathematically guaranteed results related to confidence levels using potential clouds and computed with contractors, provided that these confidence levels reflect the performances of the sensor. Therefore, our results do not ignore low-probability cases, while taking advantage of probability distributions to supplement

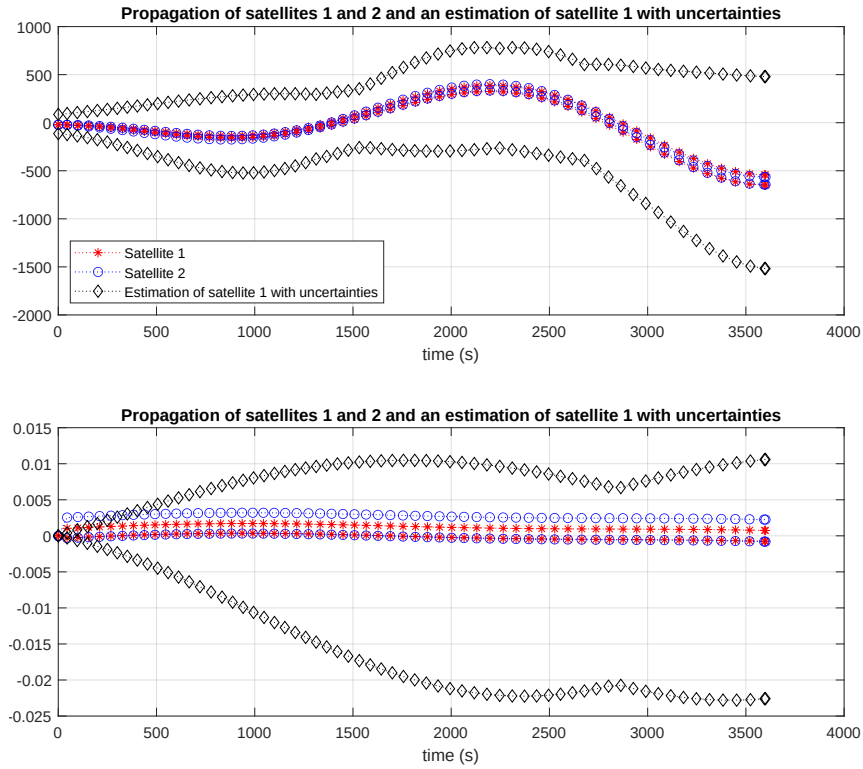

Figure 9: Centered uncertainty tubes for one hour of propagation: the tubes of satellites 1 and 2 are almost always included in the tube of the estimate of satellite 1, and always intersect with it.

the information provided by measures.

Furthermore, Monte Carlo methods require a substantial number of simulations to be reliable, compared to set-based validated methods which only need one simulation to have as much information with more guarantees. Then associated measures allow to improve the state estimate, using interval arithmetic tools such as intersection and contractors. Three scenarios showed promising results on various steps of the tracking problem, and a fourth scenario demonstrated advantages of such an approach compared to classical techniques such as NN.

As future works, implementing the retro-propagation feature of DynIbex to our algorithm would allow using the information given by a measure to reduce the uncertainty of the track beforehand. Moreover, studying the impact of a series of measures depending on the number of measures, the state of the system, the precision of the estimate and the precision of the sensor could help computing the optimal times for taking measures, to gain a maximum of information on the

system. Since operational data are available through various sources online, it would be interesting to apply our approach to such data, and then implement it on an operating ground radar. New developments could then be made in order to deal with outliers or false alarm measures which are common in this context.

References

[1] Alexandre Dit Sandretto, J. Confidence-based contractor, propagation and potential cloud for differential equations. *Acta Cybernetica*, 25(1):49–68, 2021. DOI: 10.14232/actacyb.285177.

[2] Alexandre dit Sandretto, J. and Chapoutot, A. Validated explicit and implicit Runge-Kutta methods. *Reliable Computing*, 22, 2016. URL: https://hal.science/hal-01243053/.

[3] Bar-Shalom, Y. and Tse, E. Tracking in a cluttered environment with probabilistic data association. *Automatica*, 11(5):451–460, 1975. DOI: 10.1016/0005-1098(75)90021-7.

[4] Benhamou, F., Goualard, F., Granvilliers, L., and Puget, J.-F. Revising hull and box consistency. In *Proceedings of the 16th International Conference on Logic Programming*, page 230–244. The MIT Press, 1999. DOI: 10.7551/mitpress/4304.003.0024.

[5] Blackman, S. S. and Popoli, R. F. *Design and Analysis of Modern Tracking Systems*. Artech House, 1999. ISBN: 9781580530064.

[6] Collins, J. B. and Uhlmann, J. K. Efficient gating in data association with multivariate Gaussian distributed states. *IEEE Transactions on Aerospace and Electronic Systems*, 28(3):909–916, 1992. DOI: 10.1109/7.256316.

[7] Drevelle, V. and Bonnifait, P. A set-membership approach for high integrity height-aided satellite positioning. *GPS Solutions*, 15(4):357–368, 2011. DOI: 10.1007/s10291-010-0195-3.

[8] Fortmann, T., Bar-Shalom, Y., and Scheffe, M. Sonar tracking of multiple targets using joint probabilistic data association. *IEEE journal of Oceanic Engineering*, 8(3):173–184, 1983. DOI: 10.1109/JOE.1983.1145560.

[9] Fuchs, M. and Neumaier, A. Autonomous robust design optimisation with potential clouds. *International Jorunal of Reliability and Safety*, 3:23–34, 2009. DOI: 10.1504/IJRS.2009.026833.

[10] Gill, P. E. and Murray, W. Algorithms for the solution of the nonlinear least-squares problem. *SIAM Journal on Numerical Analysis*, 15(5):977–992, 1978. DOI: 10.1137/0715063.

[11] Horwood, J. T. and Poore, A. B. Gauss von Mises distribution for improved uncertainty realism in space situational awareness. *SIAM/ASA Journal on Uncertainty Quantification*, 2(1):276–304, 2014. DOI: 10.1137/130917296.

[12] Jaulin, L., Kieffer, M., Walter, E., and Meizel, D. Guaranteed robust nonlinear estimation with application to robot localization. *IEEE Transactions on Systems, Man, and Cybernetics, Part C (Applications and Reviews)*, 32(4):374–381, 2002. DOI: 10.1109/TSMCC.2002.806747.

[13] Julier, S. J. and Uhlmann, J. K. Unscented filtering and nonlinear estimation. *Proceedings of the IEEE*, 92(3):401–422, 2004. DOI: 10.1109/JPROC.2003.823141.

[14] Mills-Tettey, G. A., Stentz, A., and Dias, M. B. The dynamic Hungarian algorithm for the assignment problem with changing costs. Technical Report CMU-RI-TR-07-27, Robotics Institute, Pittsburgh, PA, USA, 2007. URL: https://kilthub.cmu.edu/articles/The_Dynamic_Hungarian_Algorithm_for_the_Assignment_Problem_with_Changing_Costs/6561212/files/12043517.pdf.

[15] Nedialkov, N. S., Jackson, K. R., and Corliss, G. F. Validated solutions of initial value problems for ordinary differential equations. *Applied Mathematics and Computation*, 105(1):21–68, 1999. DOI: 10.1016/S0096-3003(98)10083-8.

[16] Neyman, J. Outline of a theory of statistical estimation based on the classical theory of probability. *Philosophical Transactions of the Royal Society A*, 236(767):333–380, 1937. DOI: 10.1098/rsta.1937.0005.

[17] Reid, D. An algorithm for tracking multiple targets. *IEEE Transactions on Automatic Control*, 24(6):843–854, 1979. DOI: 10.1109/TAC.1979.1102177.

[18] Rohou, S., Desrochers, B., and Jaulin, L. Set-membership state estimation by solving data association. In *2020 IEEE International Conference on Robotics and Automation (ICRA)*, pages 4393–4399. IEEE, 2020. DOI: 10.1109/ICRA40945.2020.9197039.

[19] Vallado, D. A. *Fundamentals of Astrodynamics and Applications*. Springer Science & Business Media, 2001. ISBN: 0792369033.

[20] Verhagen, S. and Teunissen, P. J. G. Least-squares estimation and Kalman filtering. In Teunissen, P. J. G. and Montenbruck, O., editors, *Springer Handbook of Global Navigation Satellite Systems*. Springer International Publishing, 2017. DOI: 10.1007/978-3-319-42928-1_22.

[21] Walker, M. J. H., Ireland, B., and Owens, J. A set modified equinoctial orbit elements (errata 1986). *Celestial Mechanics*, 36(4):409–419, 1985. DOI: 10.1007/BF01227493.